Mechanoelastic simulations of monolayer lattices of spin crossover molecules on a substrate

Anastasia Railean, Massine Kelai, Amandine Bellec, Vincent Repain, Marie-Laure Boillot, Talal Mallah, Laurentiu Stoleriu, Cristian Enachescu

Mechanoelastic simulations of monolayer lattices of spin crossover molecules on a substrate

Anastasia Railean,[1] Massine Kelai,[2] Amandine Bellec,[2] Vincent Repain,[2] Marie-Laure Boillot,[3] Talal Mallah,[3] Laurentiu Stoleriu,[1] and Cristian Enachescu[1,*]

[1]*Faculty of Physics, Alexandru Ioan Cuza University, Iasi 700506, Romania*

[2]*Université Paris Cité, CNRS, Laboratoire Matériaux et Phénomènes Quantiques, F-75013 Paris, France*

[3]*Institut de Chimie Moléculaire et des Matériaux d' Orsay, Université Paris-Saclay, CNRS, UMR 8182, 91400 Orsay, France*

(Received 19 June 2022; revised 1 November 2022; accepted 22 December 2022; published 11 January 2023)

In this paper, we discuss in the framework of a mechanoelastic model the electronic and mechanical behavior of a single layer of spin crossover molecules self-organized on a substrate. We consider the molecules situated in a face-centered-cubic structure interacting in between and with sites in the substrate by the way of connecting springs with given elastic constants. The main experimental results are reproduced, i.e., typical thermal transitions with their incompleteness of the hysteresis loop, residual fractions after low-temperature relaxations, cooperativity, or kinetic features. However, we prove that the simple model, implying fixed neighbors on the substrate for every spin crossover molecule, leads in some cases to unphysical situations, corresponding to unexpected large curvatures of the spin crossover layer. Therefore, to go further, we allow every spin crossover molecule to change its adsorption site on the substrate at every moment, by connecting to the closest molecules on the substrate. This approach, corroborated with the use of different densities of the sites on the substrate, allows us to simulate further experimental observations, such as the appearance of cracks inside the layer or periodic arrangements of apparent heights of spin crossover molecules on the layer leading to moiré patterns, for which experimental data are also provided.

DOI: 10.1103/PhysRevB.107.014304

I. INTRODUCTION

Spin crossover (SC) inorganic compounds [1] are particularly attractive due to their ability to switch between two spin states under external stimuli such as temperature, pressure, light irradiation, or applied voltage [2–4]. Their molecular switching occurs between the paramagnetic and higher entropy high-spin (HS) state, stable at higher temperature, and diamagnetic low-spin ground state (LS). Besides magnetic properties, the molecules in the two states have different volumes and optical properties. These properties make them suitable for various applications [5]. For example, recent studies demonstrated the modification of device behavior depending on the spin state of the incorporated molecules [6–9].

The subsequent miniaturization can dramatically modify their properties. Especially, for thin molecular films, the substrate used for the growth can play a major role in the switching properties [10–12]. Indeed, as demonstrated for thin films of $Fe(H_2B(Pz)_2)_2(bipy)$ (Pz = pyrazol, bipy = bipyridine) on HOPG (highly oriented pyrolytic graphite), the decrease of the film thickness from 10 monolayers to a submonolayer leads to the decrease of the transition temperature and a loss of the cooperativity [11]. In addition to that, for $Fe^{II}((3,5\text{–}(CH_3)_2Pz)_3BH)_2$ (FeMPz) molecules on metallic substrates, the epitaxial relationship between the molecular film and the underlying substrate [13] induces incomplete spin transition [14]. At low temperature, the mixture of spin state for submonolayer coverage or even single molecules has been evidenced for various couples of SC molecules and substrates [15,16]. As evidenced by scanning tunneling microscopy measurements, SC molecules can also be addressed individually but again this property is very sensitive to the interaction to the substrate [17–20]. The light transition can also be affected by the underlying substrate with the observation of anomalous light induced spin state switching for FeMPz on gold and copper [21].

Only a few models have justified the behavior of SC layers on substrates. In recent papers, Boukheddaden *et al.* studied the behavior of SC membranes deposited on deformable surfaces [22], while rPBE (revised Perdew-Burke-Ernzerhof functional) quantum chemistry calculations suggested the existence of mixtures of low-spin and high-spin molecules of Fe(II) complexes situated on a surface [23]. In other recent studies, elastic models have been used for reproducing the thermal hysteresis experiments on layers of SC materials on various substrates [14,24], the epitaxial effects [13], and the role of cooperativity [20].

Here, in order to qualitatively understand the influence of the epitaxial interactions on the behavior of a SC film deposited on a substrate, we present an extensive study of a three-dimensional mechanoelastic model applied to a single monolayer situated on a substrate.

Due to difficulties related to numerical aspects and computational time, the elastic models have been applied in most cases to 2D samples [25–29]. Only very recently, several studies referred to 3D samples of different shapes [24,30,31]. For layers composed of molecules allowed to move in all

*Corresponding author: cristian.enachescu@uaic.ro

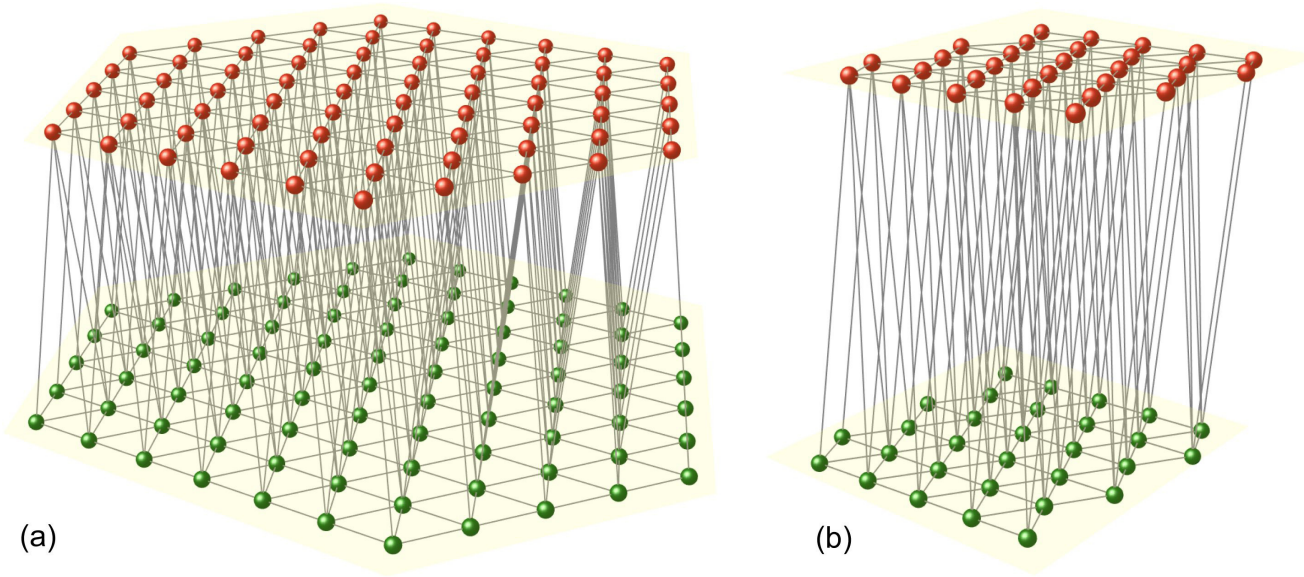

FIG. 1. Hexagonal (a) and rectangular (b) shaped samples, showing epitaxial effects, used in the simulations in their equilibrium HS state. Red spheres: HS molecules; green spheres: sites on the substrate. The size of the systems has been intentionally reduced for a better visualization.

directions, buckling effects have been observed [30], while the mechanical interactions with a substrate have been shown to be at the base of the appearance of a residual HS fraction during the thermal transition of $Fe(Pz)Pt(CN)_4$ nanoparticles adsorbed on a sapphire surface [24].

This paper focuses on epitaxial effects experienced by one single monolayer of self-assembled molecules in contact with a substrate and it is organized as follows: first, we present the basic three-dimensional mechanoelastic model and we discuss the results obtained, in terms of hysteresis and relaxation curves, residual high-spin fractions, and elastic energies. Then, considering the limits of the basic model, we adapt it for the case of smaller interactions between the SC layer and the substrate, by considering the self-adjustable choice of neighbor sites of SC molecules on the substrate and, in a further step, different densities of substrate sites comparing to the SC molecules.

II. MODEL

In the present simulations, SC molecules are represented as balls with different radii in HS and LS states, situated in the vertices of a single rectangular or hexagonal island in a triangular configuration, which are allowed to deform under the effect of the elastic energy. Each SC molecule (except those situated at edges) is linked to its six closest spin crossover molecules situated in the same layer by springs with an elastic constant k_{mol}, which modulates the cooperativity of the system. The triangular configuration has been chosen not only for a better stability of the system, but also in order to allow the use of one single elastic constant for springs connecting SC molecules. In addition, each SC molecule is linked to three substrate sites in a face-centered-cubic (fcc) configuration by springs with an elastic constant k_{sub}, which corresponds to the epitaxial effect observed in experiments [13]. The manner in which SC molecules are connected in between and with the substrate is presented in Fig. 1, for both hexagonal and rectangular situations.

The simulations in the present paper are performed for spin crossover layers composed of 70–24 210 molecules in triangular configuration with hexagonal or rectangular shape; the substrate has the same shape as the SC layer, but is one line larger on each side, to ensure that all SC molecules, including those on the edges are linked with three substrate sites. The equilibrium state corresponds to a situation when all SC molecules are in the HS state (which means that the configuration of the substrate is equivalent with that of a fully HS SC layer). In this situation, all springs have their natural length—they are neither compressed nor elongated.

The Hamiltonian for the elastic model can be simply written as [26]

$$H = \frac{1}{2}\sum_i (D - k_B T \ln g)\sigma_i + \frac{k}{2}\sum_{i,j} \delta x_{ij}^2, \qquad (1)$$

where σ_i is the spin state of the ith molecule, the first term corresponds to the Gibbs free energy of the system (D is the HS $\rightarrow$ LS energy difference and can be regarded as the difference in enthalpy between the two states in the case of noninteracting molecules; g is the vibronic degeneracy ratio between the HS and LS states such that $k_B \ln g$ corresponds to the difference in entropy between them two states), and the second term stands for the elastic energy (k is equal to either k_{mol} or k_{sub}) calculated as the sum of energies for all the springs (including springs between spin crossover molecules and substrate) in the system.

The material parameters used in the present paper, $D = 1500 \times 10^{-23}$ J, $g = 1096$ (which corresponds to an entropy difference between the states equal to 9.7×10^{-23} J/K), giving a thermal transition for the bulk centered around 155 K, are in line with standard experimental calorimetric data for Fe(II) spin crossover systems [32,33] and are similar to those

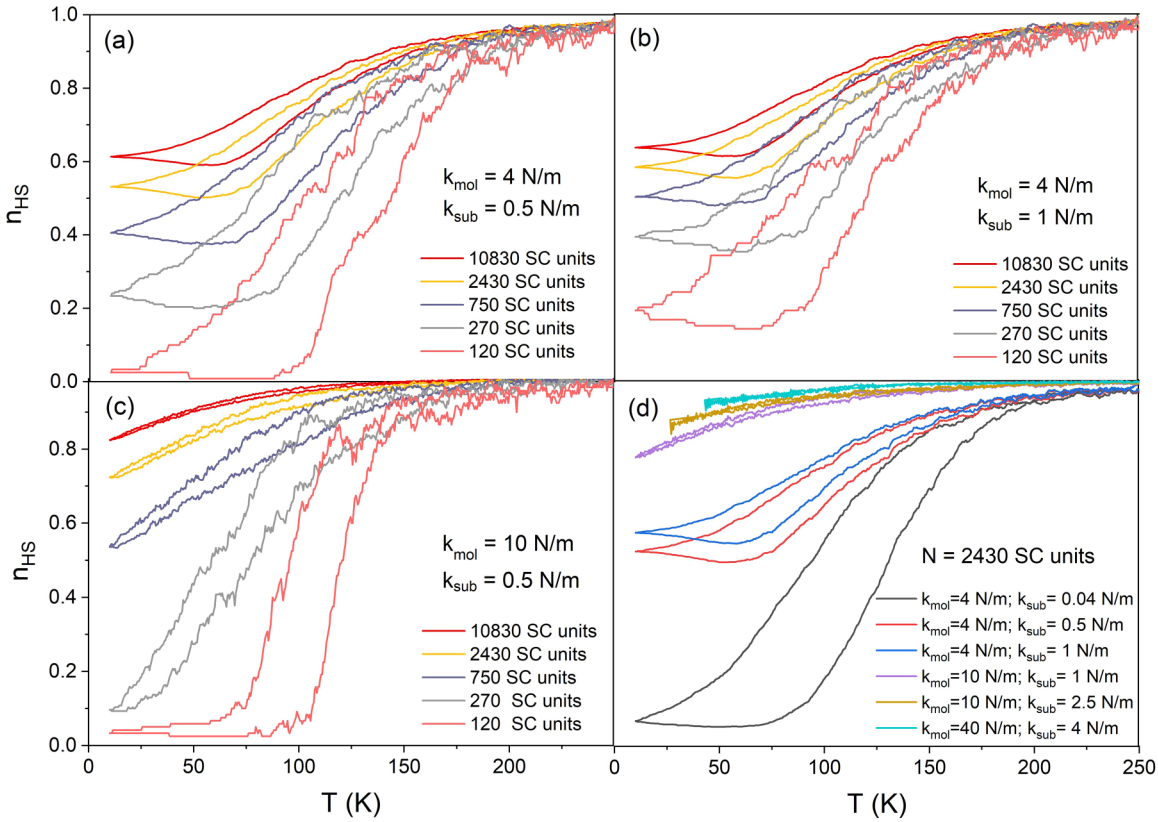

FIG. 2. Thermal hysteresis for different sizes of rectangular-shaped SC layers situated on substrates. $k_{\mathrm{mol}} = 4$ N/m [(a), (b)], $k_{\mathrm{mol}} = 10$ N/m (c), $k_{\mathrm{sub}} = 0.5$ N/m [(a), (c)], $k_{\mathrm{sub}} = 1$ N/m (b). Direct comparison of k_{mol} and k_{sub} effects in the case of a system composed of 2430 molecules (d).

used in other mechanoelastic approaches of spin crossover systems. Spin crossover molecules in their HS state and surface molecules have a radius of 0.22 nm, while molecules in the LS state have a radius of 0.20 nm. The distance between centers of molecules is 1 nm in the LS state (1.04 nm in the HS state)—which means that the springs have an uncompressed length of 0.6 nm. These values correspond to x-ray experimental measurements for typical spin crossover systems [32,33].

The evolution of the system is then described through Monte Carlo Arrhenius dynamics, in which the transition probabilities are modulated by the activation energy barrier of the HS → LS relaxation E_a (600×10^{-23} J), which is considered as relative to a global reference state in which all the molecules are in the HS state. In this approach the transition probabilities can be written [27]

$$P^i_{HS\to LS} = \frac{1}{\tau}\exp\left(\frac{D - k_B T \ln g}{2k_B T}\right)\exp\left(-\frac{E_a - \kappa p_i}{k_B T}\right),$$
$$P^i_{LS\to HS} = \frac{1}{\tau}\exp\left(-\frac{D - k_B T \ln g}{2k_B T}\right)\exp\left(-\frac{E_a + \kappa p_i}{k_B T}\right), \tag{2}$$

where τ is a scaling constant (here 1000), chosen so that the above probabilities are well below unity at any temperature, and p_i is the local pressure force (measured in N) acting on molecule i, defined as

$$p_i = \sum_{\text{neighbor springs}} k\,\delta x_{ij}, \tag{3}$$

with δx_{ij} taken positive for compressed springs and negative for elongated ones, and κ is a scaling factor between the local pressure and the activation energy of the individual molecule and takes the value 1450×10^{-14} J/N, similar to that used in previous studies [34].

The simulation is realized in two steps. First, in a Monte Carlo step (MCS), we compute the switching probabilities according to Eq. (2) for all molecules in the system and we compare them with random numbers generated in the range (0, 1). If a transition probability for one particular molecular switch is higher than the corresponding random number, then the switching is accepted and the molecule flips to the new state; otherwise, the molecule keeps it previous state. Different radii of HS and LS SC molecules will result in a compression or elongation of neighboring springs, which is transmitted throughout the sample as an elastic wave. In a second step, after every MCS, the position of all molecules in the system is updated by solving a system of differential equations which takes into account the pressure forces determined by the elongations of the springs for every molecule in the system [25]. The final positions of molecules correspond to the mechanical equilibrium; i.e., the resultant force on every molecule is zero.

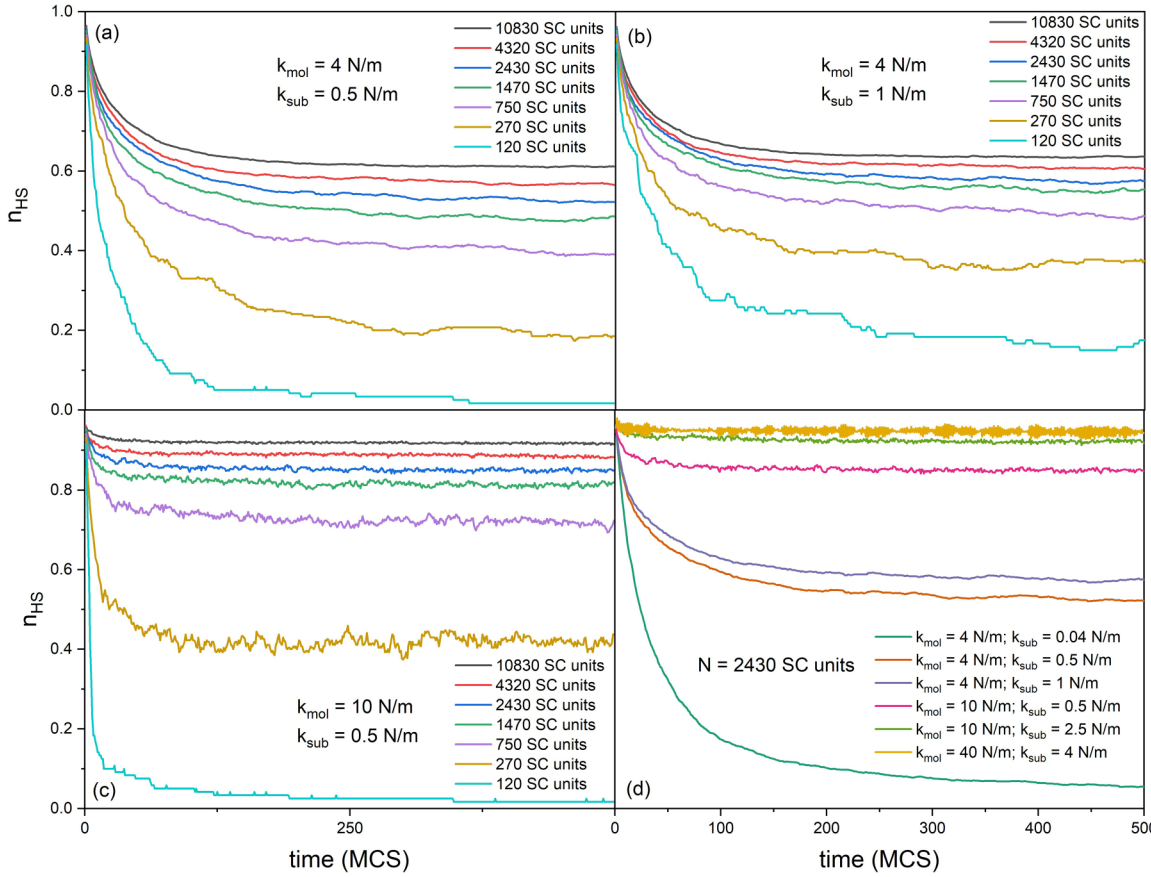

FIG. 3. Relaxation curves for different sizes of the spin crossover layer, for intermediate values of k_{mol} ($k_{\mathrm{mol}} = 4$ N/m) [(a), (b)] and k_{sub} ($k_{\mathrm{sub}} = 1$ N/m) (a) or large k_{mol} ($k_{\mathrm{mol}} = 10$ N/m) (c) and small k_{sub} ($k_{\mathrm{sub}} = 0.5$ N/m) [(b), (c)]. Relaxation curves for a system composed of 2430 SC molecules for different k_{mol} and k_{sub} values (d).

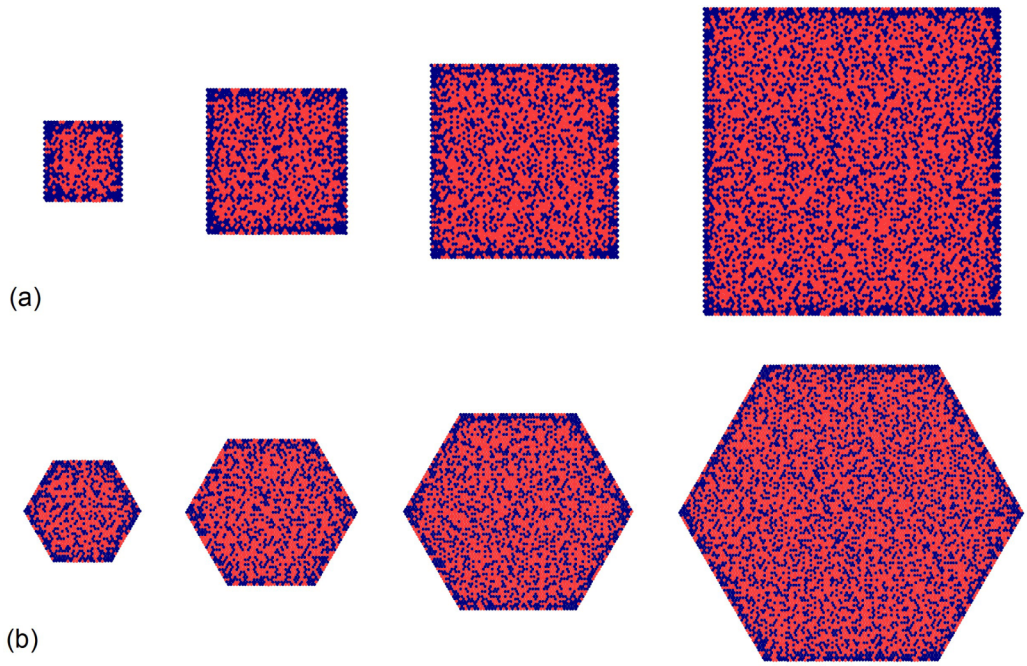

FIG. 4. Snapshots of the SC layer (top view) in the steady state after relaxation for different sizes for rectangular-shaped layers (a) (750, 2430, 4320, 10 830 units from left to right) and hexagonal-shapes layers (b) (660, 1261, 4760, 10 740 units from left to right). Scale not respected. Blue circles: LS molecules; red circles: HS molecules. Moderate interactions in between molecules and with the substrate have been considered ($k_{\mathrm{mol}} = 4$ N/m and $k_{\mathrm{sub}} = 1$ N/m).

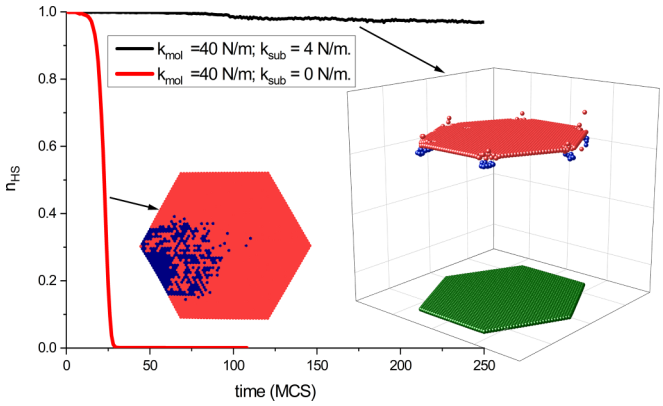

FIG. 5. Relaxation curves for a high cooperative system composed of 2791 molecules ($k_{\rm mol} = 40$ N/m) situated on a substrate ($k_{\rm sub} = 4$ N/m) and as a free 2D system. Insets: Snapshots of the final stationary state for the layer on the substrate showing stable LS clusters and of a transitory state ($n_{HS} = 0.5$) for the 2D system showing an avalanche phenomenon.

III. RESULTS AND DISCUSSION

A. Size effects and role of elastic constants

First, we have computed thermal hysteresis for SC rectangular-shaped layers of different sizes situated on substrates, considering different cooperativities ($k_{\rm mol}$) and elastic interactions ($k_{\rm sub}$) with the sites on the substrate. Even if recent experimental studies show that the bulk modulus is state dependent, [37,38], for the sake of simplicity we have considered here a unique value for $k_{\rm mol}$, irrespective to the state. In the Appendix, we present the effects of using state-dependent elastic constants, with a larger elastic constant for springs connecting LS states, which only slightly affect the simulated curves. From the results presented in Fig. 2, we can notice the influence of these parameters and of the system size on the width and the shape of the hysteresis loop, as well as

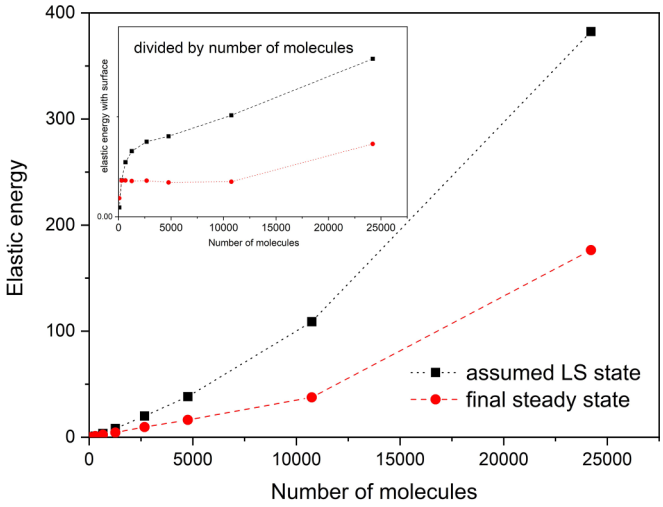

FIG. 6. Elastic energy between SC units (main figure) and elastic energy with the surface (inset) for moderate values of $k_{\rm sub} = 1$ N/m, $k_{\rm mol} = 4$ N/m, for the steady states corresponding to relaxation curves in Fig. 3 (circles) and for forced fully LS states (squares).

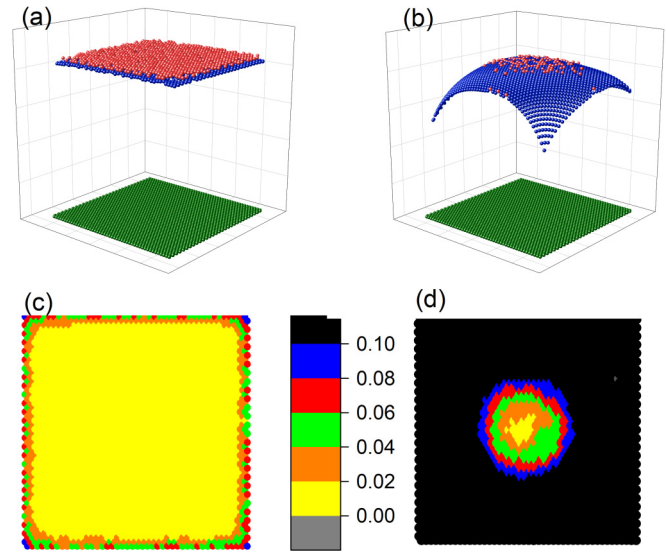

FIG. 7. Snapshots of the system (side view) for a system composed of 2430 molecules for $k_{\rm sub} = 1$ N/m (a) and $k_{\rm sub} = 0.04$ N/m (b) with $k_{\rm mol} = 4$ N/m. Map of relative elongations of springs connecting SC molecules with the substrate for $k_{\rm sub} = 1$ N/m (c) and $k_{\rm sub} = 0.04$ N/m (d).

on the residual HS fraction. The increase of the strength of substrate-monolayer interactions translates into larger residual high-spin fractions [Fig. 2, panels (a), (b), (d)]. This situation is due to the shrinking of the layer while molecules switch from larger volume HS to lower volume LS state, which produce larger elastic forces between SC layer and the substrate. These forces, directly depending on the value of the elastic constant of the springs linking SC molecules to substrate molecules, gradually decrease the HS $\rightarrow$ LS transition probabilities with every molecule switching from HS to LS state. A similar description was previously used for explaining the larger residual HS fraction observed in spin crossover molecules embedded in matrices [35,36]. The strengthening of intralayer cooperativity produces the same effect [Fig. 2, panels (a), (c), (d)] [14]. As the system size increases, larger high-spin fractions are obtained, irrespective of $k_{\rm mol}$ and $k_{\rm sub}$ values.

It is well known that the Monte Carlo simulated hysteresis loops are influenced by kinetic effects [39], and thus the temperature sweeping rate, which can also play an important role for the residual fraction, has to be considered. To overcome limitations in the computational time that increases for small temperature sweeping rate, in the following we rather simulate relaxation curves which can provide valuable information in a straightforward way.

Relaxations for systems with the sizes between 120 and 10 830 molecules at 60 K are plotted in Fig. 3. In Fig. 3, panels (a), (b), (c), we considered either intermediate values of $k_{\rm mol}$ ($k_{\rm mol} = 4$ N/m) and $k_{\rm sub}$ ($k_{\rm sub} = 1$ N/m) or large $k_{\rm mol}$ ($k_{\rm mol} = 10$ N/m) and small $k_{\rm sub}$ ($k_{\rm sub} = 0.5$ N/m). The $k_{\rm mol}$ values are similar to those used in previous papers dealing with the effect of a substrate on hexagonal spin crossover layers [13,14,20,24], slightly smaller than those estimated by the DFT-U calculations [13]. In Fig. 3(d), we show various relaxation curves for a system composed of 2430 molecules.

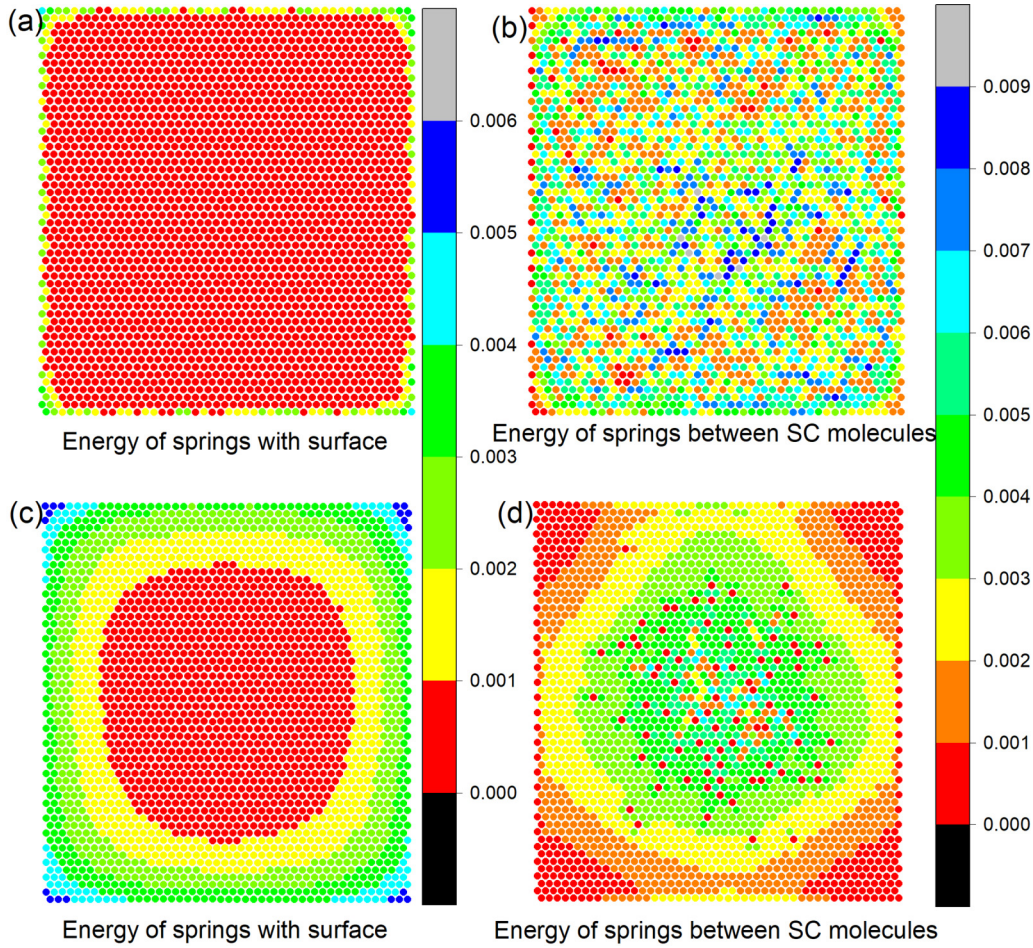

FIG. 8. Representation of elastic energies at every site, for a system composed of 2430 molecules, as the energy of springs linking SC molecules with the substrate [(a), (c)] and as the elastic energies of springs linking spin crossover molecules [(b), (d)] for $k_{sub} = 1$ N/m [(a), (b)] and $k_{sub} = 0.04$ N/m [(c), (d)] with $k_{mol} = 4$ N/m. Red circles: Small values; blue circles: large values.

Basically, the same aspects as in the case of the hysteresis loops may be noticed: for smaller systems the relaxation is complete in all situations while a residual fraction appears and then increases with the size of the system, converging to a limit, with the value depending on the cooperativity and the interaction with the substrate [Fig. 3, panels (a), (b), (c)]. For larger k_{sub} and k_{mol}, the residual HS fraction increases [13], and in order to obtain a residual fraction close to unity, a very large value of the k_{mol} should be considered ($k_{mol} = 10$ N/m) [Fig. 3(d)].

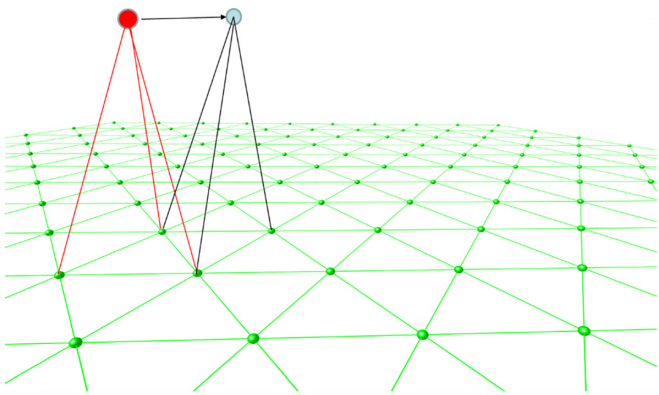

FIG. 9. After every step the spin crossover molecule is connected with the three closest sites on the substrate.

In order to understand the microscopic behavior of the SC molecules, it is useful to visualize the snapshots of the system corresponding to final steady states, which we display in Fig. 4, for rectangular-shaped systems and, for comparison purpose, for hexagonal-shaped systems for moderate k_{mol} ($k_{mol} = 4$ N/m) and k_{sub} ($k_{sub} = 1$ N/m). For rectangular systems, the residual HS fractions correspond to those in Fig. 3(a). We notice that the SC molecules situated at the edges are more susceptible to switching to the LS state, because of the natural cluster development from the edges or corners [40], but also to the larger flexibility of the lattice at edges which results in the possibility to get closer to the substrate and thus to reduce the pressure forces from the substrate. At the same time, the central parts of all systems present similar proportions of HS and LS molecules. Therefore, the dependence of the residual fraction on the size shown in Fig. 3, panels (a), (b), (c), is at least partly determined by the ratio between the number of SC molecules situated at the edges and the total number of SC molecules in the layer.

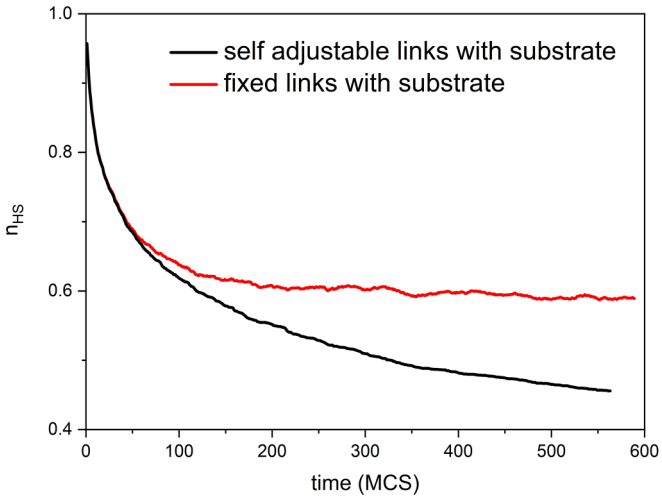

FIG. 10. Comparison of relaxations curves, for a hexagonal-shaped lattice with 2670 molecules for two systems with fixed links between SC molecules and the substrate and with flexible links in the case of moderate $k_{mol} = 4$ N/m and $k_{sub} = 0.04$ N/m values.

Here it is instructive to compare the behavior of a SC layer on a substrate, with a 2D plane hexagon, without any constraints from a substrate (Fig. 5 and inset of Fig. 5), where the transition is driven by formation of clusters from the edges, subsequently showing an avalanche-type switching, in the case of a high cooperativity (here $k_{mol} = 40$ N/m and $k_{sub} = 1$ N/m) [40]. In the case of a system linked to a substrate, the first nucleation germs are equally formed near corners, but the effect of the substrate prevents their further development toward the bulk, which remains mostly in HS state. A steady state is then produced, with a well-defined HS residual fraction.

The total elastic energies between spin crossover units for the moderate k_{sub} and k_{mol} values are presented in Fig. 6 (red symbols). We notice that they increase with the number of involved sites, both in absolute values and in values corresponding to one single molecule. For comparison, we present together the total elastic energy of a supposed LS state (for this representation, the spin crossover units are forced to the LS state and then the elastic energy is calculated after they relax to the lower energy state). The difference between the two energies is relatively small for small systems, but dramatically increase in the case of very large systems; that is why it is more difficult to obtain the complete relaxation to the LS ground state for large systems. Actually, a simple analytical calculation in the case of a spin crossover chain situated on a substrate considered fixed on Z axis shows that for a full switching to the LS state, the elongation of springs linking edge molecules of the chain to the substrate would be larger than 10% if the length of a chain surpasses 45 sites (considering the bending of the chain or a 2D layer would change this value, but the underlying problem will be similar). In simulations, this situation must be avoided as it surpasses the limits of harmonic approximation. Certainly, strong interactions between substrate and SC layer would not allow such large spring elongations (and this is actually the main reason for which the transition is not complete), but in the case of lower interactions, this may happen, as we discuss in the following paragraphs.

Therefore, we have to establish the conditions in which the system keeps its physical meaning. Let us explore in the following the influence of the k_{sub} value on the behavior of the SC layer. In Figs. 7(a) and 7(b) we represent snapshots corresponding to steady state after relaxation for a moderate $k_{sub} = 1$ N/m and a small $k_{sub} = 0.04$ N/m, while keeping $k_{mol} = 4$ N/m. Due to the fact that SC molecules reduce their volume during the switch from HS to LS state (while substrate sites are fixed), the whole SC layer will reduce its size during relaxation and the elongation of the springs will increase. In order to keep the total elastic energy to a minimum, the SC layer becomes distorted. As explained above, the SC layer is more distorted in the case of small k_{sub} constant, as the smaller spring constant with the substrate allows the spin crossover molecules to move relatively free on the Z axis, while in the case of a strong coupling with the surface the elastic energy stored in springs would be too large if SC molecules approach the substrate. This is in agreement with data presented before for multiple layers of spin crossover nanoparticles [24], where it was shown that for a free system a minimum energy state is obtained when a switched molecule moves outside its initial plane (the so-called buckling effects), and the size of the lattice on the XY plane does not practically change as the deformation is transferred to the Z axis.

In the same time, the motion of molecules on the Z axis influences the length of the springs, as one can see in Figs. 7(c) and 7(d). If in the case of moderate k_{sub} the relative change in length is low (under 10%), in the case of low value of k_{sub} most of springs connecting SC molecules with the substrate change dramatically their length from 10% to almost 50%. This change is larger in the case of molecules situated along edges, and only SC molecules very close to the center of the layer are not affected. Consequently, the use of a too low k_{sub} value leads in the framework of this model to unphysical situations and must be avoided.

A further insight to this situation is provided by the comparison, in Fig. 8, of the elastic energies for the two systems. For this, we have to distinguish between elastic energies of springs linking spin crossover molecules and of springs linking sites with the substrate. Due to the deformation of the SC layer, the elastic energy stored inside the springs will increase. While in the case of moderate ratio, the distribution of energies is quite homogeneous (with somewhat higher values of the SC-substrate energies for molecules situated at the border, as they move more), for small ratio, the situation of energy distribution is different. As explained above, the edge SC molecules needed to move more (because of the lower HS fraction), and their energy with the substrate is considerably higher than that of bulk molecules. However, the elastic energy between molecules is smaller around corners than in the bulk, which is in line to the energy of a cluster starting form a corner in 2D systems [40–43].

As a conclusion, we should be aware that a too large (i.e., a hundred times) ratio between k_{mol} and k_{sub} leads to an exceptional variation of the length of springs connecting edge

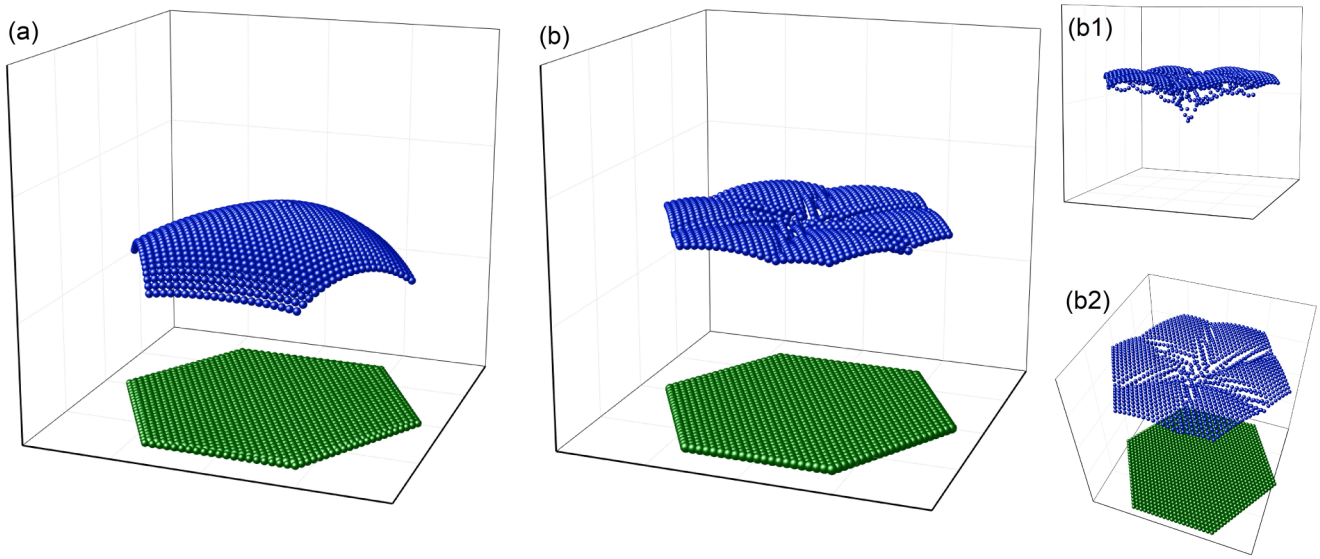

FIG. 11. System showing large local distortion for a system of hexagonal shape with flexible links composed of 2670 molecules for $k_{sub} = 0.04$ N/m [(b), with zooms in (b1) and (b2)] and comparison with a system with fixed links (a).

SC molecules with the substrate, which exceeds the present harmonic hypotheses of the mechanoelastic model. Therefore, in the following we propose an alternative method for dealing with such situations.

B. Extended model considering self-adjustable interactions

As we have previously discussed and represented in Fig. 7(b), in the case of small k_{sub}, the curvature of the spin crossover layer is extremely large. Particularly in the case of large systems, for a complete transition, the horizontal projection of the distance between the SC molecules and their linking substrate sites is very large. That is why for large k_{sub} the system is stuck with a high HS residual fractions (the elastic energy in a case of a distorted system in order to allow the complete transition will be too high), while for lower k_{sub} the edges of the system are approaching the substrate.

In order to prevent this behavior, instead of considering for every SC molecule three fixed neighbors on substrate, we assume the presence of self-adjustable interactions between the SC molecules and the substrate. For this, at every moment we choose as neighbor sites, the three closest sites on the substrate for every molecule. Consequently, an additional step is added to the algorithm: after every Monte Carlo step, we determine which are the closest three sites on the substrate for every SC molecule and (re)connect this molecule with them, as we can see in Fig. 9.

The immediate effect of this procedure on the relaxation curves can be seen in Fig. 10. As the system has more flexibility now, more HS spin crossover molecules will relax toward the LS state, for the same values of the parameters of the system. In the first one hundred MC steps or so, the relaxation curves are quite similar, as the lattice size changed very little and few SC molecules changed their linked sites, but the difference increases as approaching the steady state.

However, this procedure may affect the stability of the system and lead to the appearance of cracks. Certainly, the too large curvature of the SC layer is eliminated (Fig. 11), but local distortions can be very large because several SC molecules on the layer have the same corresponding sites on the substrate [inset of Fig. 11(b)].

This is not completely unexpected, as experimentally cracks can sometimes be observed in molecular islands. Figure 12 presents an example of such phenomena on a self-assembled molecular island of one-monolayer FeMPz sublimated at 358 K on a Au(111)/mica substrate kept at room temperature and imaged at 200 K.

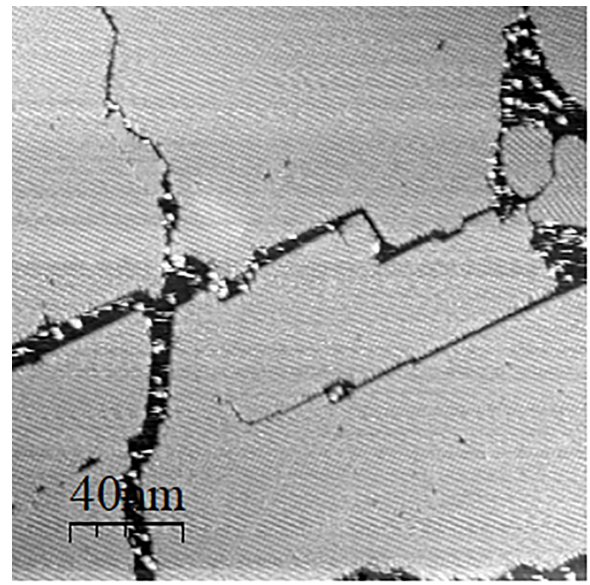

FIG. 12. 200×200 nm^2 STM topographic image of one monolayer of FeMPz molecules adsorbed on Au(111)/mica at 200 K ($V = 0.3$ V, $I = 20$ pA).

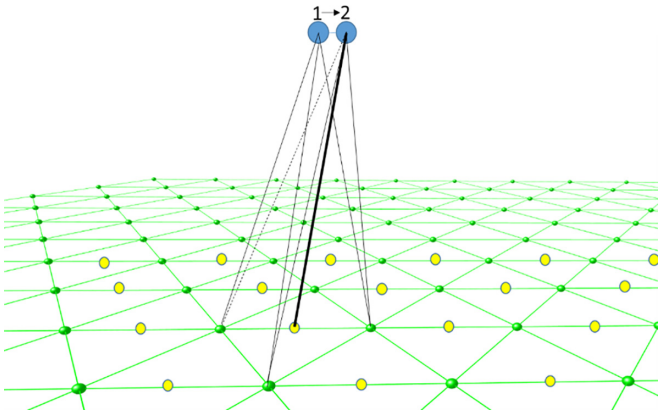

FIG. 13. Change of the substrate interacting sites of a SC molecule is facilitated by a larger density of interacting sites on the substrate.

C. Self-adjustable interactions and different density of sites on substrates

The presence of cracks in simulations is determined by the fact that, following the size reduction during the transition, several SC molecules will have the same neighbor sites, which lead to increasing the local pressure. In a further step, we may assume that the density of substrate sites (or even the structure of the substrate) is different than that of the SC lattice, which is justified as the substrate and the lattice are formed from different materials. In this case, the pressure on the spin crossover molecules is released as they may choose between different interacting sites on the substrate (Fig. 13).

A first effect, visible in Fig. 14, is that, with k_{sub} and k_{mol} kept constant, both the relaxation kinetics and the residual fractions depend on the density of interacting sites (i.e., the ratio of the distance between the neighboring sites on the substrate and the distance between neighboring SC molecules);

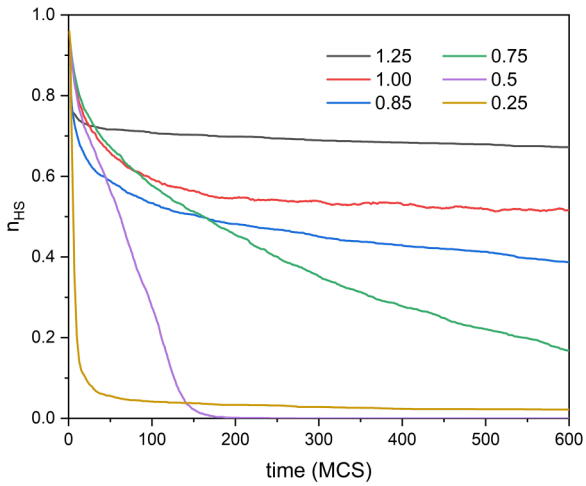

FIG. 14. Comparison of relaxations, for different ratios r between the linear densities of the SC molecules and substrate sites ($r = 1.25$ to 0.25) for a rectangular system composed of 2430 molecules with self-adjustable interactions between SC molecules and the substrate ($k_{\mathrm{sub}} = 1$ N/m, $k_{\mathrm{mol}} = 4$ N/m).

a larger density of sites on the substrate implies more flexibility of the system and less constraints. Indeed, in this case, SC molecules will be able to change easier their substrate neighbors with a lower cost of elastic energy and therefore more energy will be available for the transformation of HS to LS states. However, by changing the interaction with the substrate, a residual HS fraction can be obtained again, at the same value as in previous cases. The hysteresis loop, shown in Fig. 15(a) for a system composed of 2430 molecules system with adjustable interactions, show a complete vanishing of the residual HS fraction.

An important difference determined by a larger density of interaction sites on the substrate is the absence of large local or global distortions. One can notice the existence of periodical arrangements on the position of molecules on Z axis [Figs. 15(b) and 15(e)]; the period depends on the value of the interaction with the substrate and on the distance between interaction centres as in the classical 1D Frenkel-Kontorova model [44], showing the self-organization of stresses with the surfaces [45]. In Figs. 15(c) and 15(d) we present the building up of the LS states during the HS $\rightarrow$ LS transition for different values of n_{HS}, showing that moiré patterns start to form just below $n_{HS} = 0.5$. We notice that at early stages of the transition, if a molecule has switched to the LS state, it approaches the substrate; however, as the transition proceeds some molecules become closer to the substrate than others and thus the periodic arrangement of heights of molecules is created.

By this approach, it would be possible to simulate interactions with substrates having different structures comparing with the spin crossover layer, with the only concern to determine, for every SC molecule and at every moment, three interacting sites on the substrate.

Experimentally, moiré patterns can be observed by STM over nanometric FeMPz islands adsorbed on Cu(111) or on HOPG substrates as visible in Fig. 16. Here the two samples have been annealed at room temperature after sublimating the molecules on the substrate kept at 5 K. The periodic buckling of molecules in the 3D mechanoelastic model displayed in Fig. 15(e) could be at the origin of the observed moiré patterns.

For a deeper understanding of the simulated moiré patterns, in Fig. 17, we analyze the impact of the ratio r between the linear densities of SC and substrate sites. All the snapshots correspond to fully LS states. A small enough ratio (larger densities of sites on the substrate) allows the SC molecules to easily find new neighbors on the substrate when the SC layer shrinks; therefore smaller displacements of SC molecules on the Z axis will be necessary and the moiré patterns will present a smaller period. With the considered parameters, moiré patterns can be observed for $r = 1/2$ and $1/3$. Patterns with a very small amplitude and small periods are also observed for $r = 1/4$. Larger distance (r ratio exceeding $2/3$) between substrate sites makes inefficient the periodic arrangements of SC molecules and the moiré patterns disappear (as in the case treated in the first part of this paper with the same density of SC molecules and substrate sites). In addition, we have represented in Fig. 18 the influence of the elastic constants k_{mol} and k_{sub} on the appearance of moiré patterns, by keeping the same ratio $(1/2)$ between the density of substrate sites

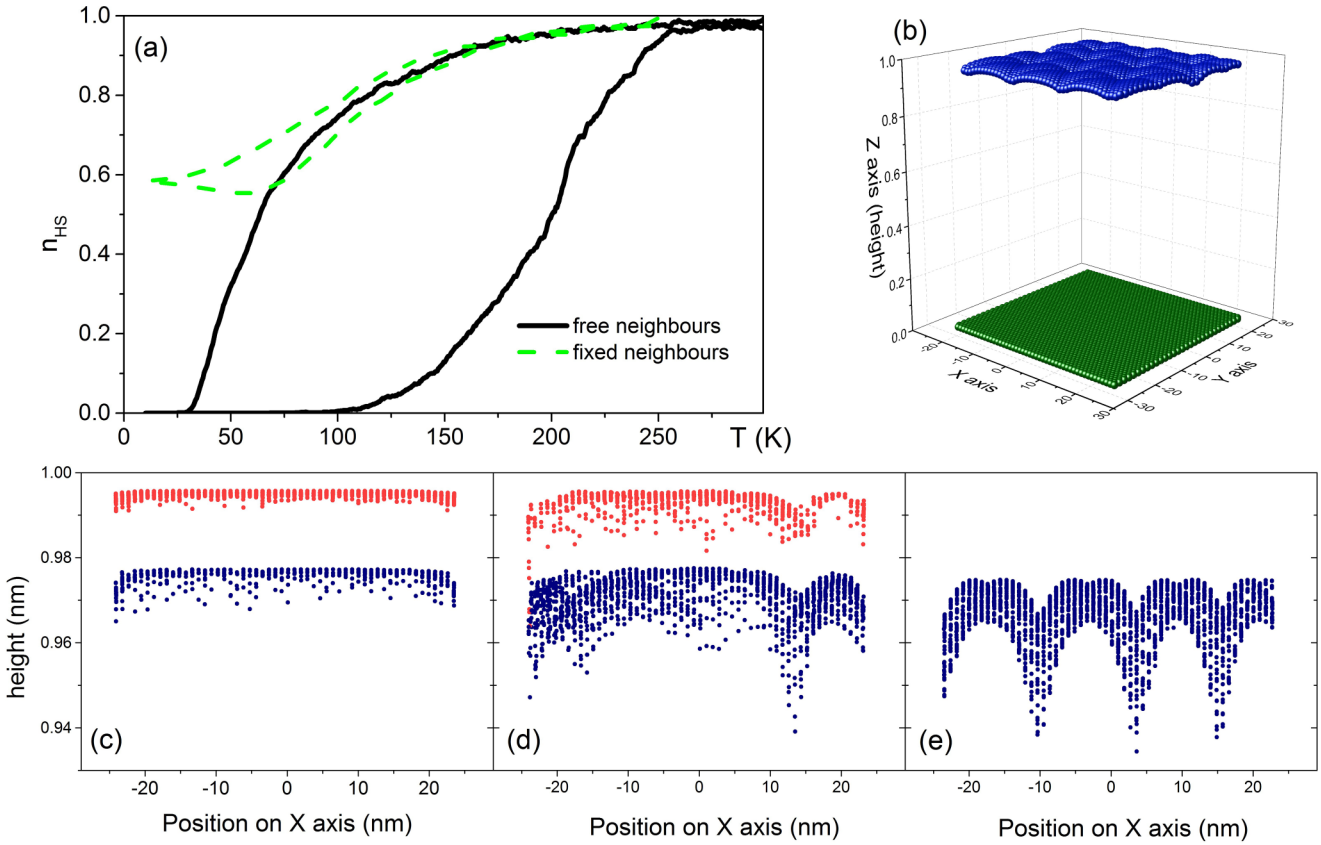

FIG. 15. (a) Hysteresis loop for a system composed of 2430 molecules with self-adjustable interactions between SC molecules and the substrate (flexible neighbors) ($k_{\text{sub}} = 1$ N/m, $k_{\text{mol}} = 4$ N/m) for a 1/2 ratio between the densities of SC molecules and substrate sites and comparison with the hysteresis for the same system with fixed neighbors (shown in Fig. 2). (b) Snapshot of the system with flexible neighbors in its final state. (c), (d), (e) The displacements of molecules on Z axis seen from Y axis for $n_{HS} = 0.7$, $n_{HS} = 0.4$, and $n_{HS} = 0$, respectively. Blue circles: LS molecules. Red circles: HS molecules.

and SC molecules. We notice that, as far as the k_{mol} is much larger than k_{sub}, the moiré patterns are preserved without any visible change, both in periodicity and in amplitude. This is due to the fact that the elastic energies between SC layer and substrate are much smaller than those inside SC layer, which allows the relatively free arrangements of SC molecules on the Z axis. As soon as the k_{sub} value approaches k_{mol}, the period of arrangement of SC molecules starts to increase and finally for k_{mol} equal to k_{sub}, the periodicity completely disappears, as the elastic energies between SC molecules are comparable to those between SC molecules and substrate.

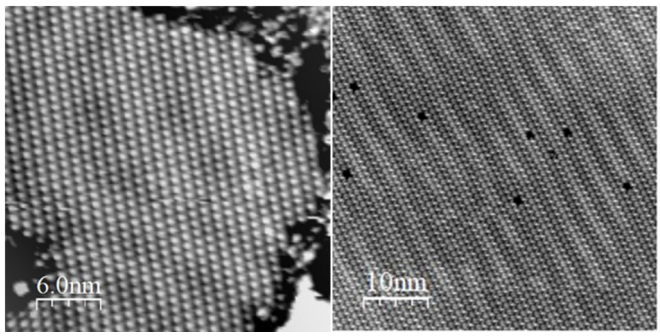

FIG. 16. (a) 30×30 nm^2 STM topographic image of a domain of FeMPz molecules grown on Cu(111) ($V = -1.5$ V, $I = 20$ pA, 5 K). (b) 50×50 nm^2 STM topographic image of FeMPz island grown on HOPG ($V = -2$ V, $I = 10$ pA, 5 K).

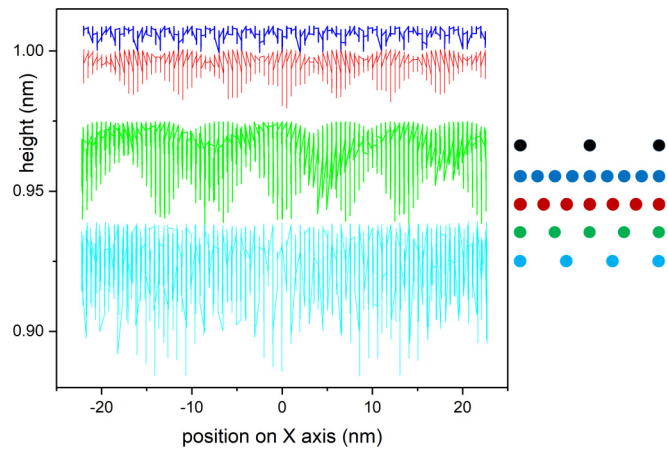

FIG. 17. The effect of the ratio between the linear densities of SC molecules and substrate sites on moiré patterns. k_{mol} (4 N/m) and k_{sub} (1 N/m) were kept constant. On the right side of the figure we have schematically represented the distance between SC molecules (black circles) and the distance between substrate sites, corresponding to linear ratios $r = 1/4$, 1/3, 1/2, and 2/3 of the curves presented in the lift side. In all cases, the relaxations are complete.

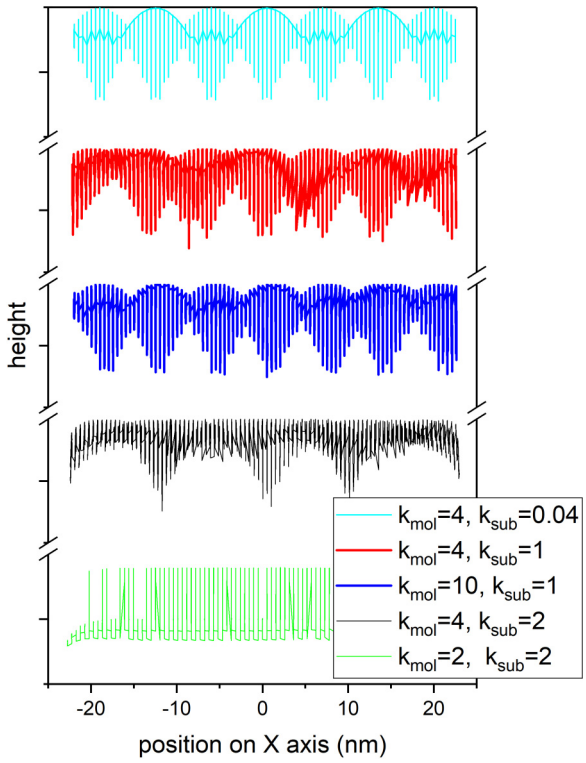

FIG. 18. The effect of spring constants on moiré patterns for the same ratio (1/2) between the linear density of SC molecules and substrate sites. The relaxations are complete in the first three situations and almost complete (final $n_{HS} = 0.01$ and $n_{HS} = 0.08$) for the two bottom curves.

IV. CONCLUSIONS

In this paper, we have reproduced the behavior of a layer of spin crossover (SC) molecules situated on a substrate by the way of a three-dimensional mechanoelastic model. We have reproduced the existence of residual HS fractions and studied their dependence on the system size, on the intrinsic cooperativity of SC system, and on interactions between SC molecules and substrate. We have shown the drawbacks of the simple model, which could lead to nonphysical situations for small values of interactions with the substrate, and we presented possible improvements, as accounting for self-adjustable interactions between the spin crossover molecules and the substrate, which allow the permanent change of the neighbor sites on the substrate. The simulations realized in this paper could be useful for the design and the understanding of future experiments and applications implying spin crossover films, as well as for the understanding of other systems showing epitaxial effects. The research should further deal with the use of different structures of the substrates, opening the possibility for considering different patterns for *OX* and *OY* axes of the substrate and anisotropic effects and also should approach the reciprocal influence of the spin crossover molecules and the sites of the substrate.

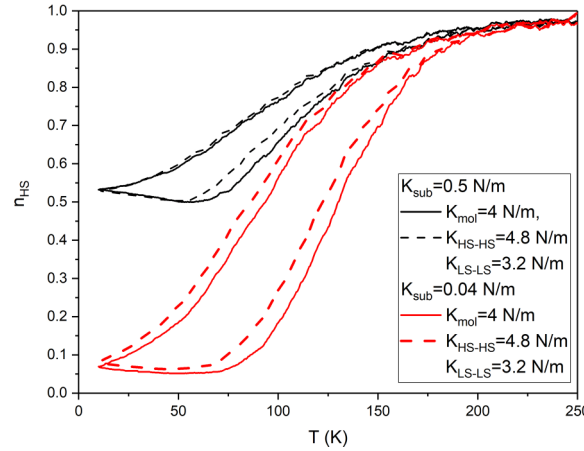

FIG. 19. The effect of different spring constants between HS-HS and LS-LS molecules for moderate k_{mol}, with two extreme cases $k_{\mathrm{sub}} = 0.04$ and $k_{\mathrm{sub}} = 0.5$ N/m1. The full lines correspond to those presented in Fig. 2.

ACKNOWLEDGMENTS

This work was supported by a grant of the Romanian Ministry of Education and Research, CNCS-UEFISCDI, Project No. PN-III-P4-ID-PCE-2020-1946, within PNCDI III. The team has received funding from the European Union's Horizon 2020 research and innovation program under Grant Agreement No. 766726. The collaboration between the Iasi and Orsay teams has been supported by the PHC Brancusi program. C.E. gratefully acknowledges hospitality, as invited professor, at Université Paris Diderot (now Université Paris Cité).

APPENDIX

In this paper, we have used a single value for the elastic constant between SC molecules. Since in recent experimental papers, a difference of 25%–50% between the elastic constant of springs linking HS molecules and those connecting LS molecules [37,38] has been observed, we have tested here the effect of considering different elastic constants for springs connecting HS to HS molecules and springs connecting LS to LS molecules (with an average value for springs connecting HS to LS molecules). In Fig. 19 we present this effect for the case of a moderate k_{mol} with low and high values k_{sub} and some (small) differences can be observed (a slower decrease of the HS fraction while descending temperatures and a faster increase during the ascending hysteresis branch). However, qualitatively the curves stay the same—and since we are interested here only in a qualitative model, we have preferred to use the minimum of parameters and a single elastic constant.

[1] M. A. Halcrow, *Spin-Crossover Materials: Properties and Applications* (John Wiley & Sons, Chichester, UK, 2013).

[2] C. Lefter, S. Rat, J. S. Costa, M. D. Manrique-Juarez, C. M. Quintero, L. Salmon, I. Seguy, T. Leichle, L. Nicu, P. Demont,

A. Rotaru, G. Molnar, and A. Bousseksou, Adv. Mater. **28**, 7508 (2016).
[3] E. J. Devid, P. N. Martinho, M. V. Kamalakar, I. Salitros, U. Prendergast, J. F. Dayen, V. Meded, T. Lemma, R. Gonzalez -Prieto, F. Evers, T. E. Keyes, M. Ruben, B. Doudin, and S. J. van der Molen, ACS Nano **9**, 4496 (2015).
[4] O. I. Utesov, S. Burdin, P. Rosa, M. Gonidec, L. Poggini, and S. V. Andreev, Phys. Rev. B **100**, 235126 (2019).
[5] G. Molnár, S. Rat, L. Salmon, W. Nicolazzi, and A. Bousseksou, Adv. Mater. **30**, 1703862 (2018).
[6] J. Dugay, M. Aarts, M. Gimenez-Marques, T. Kozlova, H. W. Zandbergen, E. Coronado, and H. S. J. van der Zant, Nano Lett. **17**, 186 (2017).
[7] N. Konstantinov, A. Tauzin, U. N. Noumbe, D. Dragoe, B. Kundys, H. Majjad, A. Brosseau, M. Lenertz, A. Singh, S. Berciaud, M. L. Boillot, B. Doudin, T. Mallah, and J. F. Dayen, J. Mater. Chem. C **9**, 2712 (2021).
[8] E. P. van Geest, K. Shakouri, W. Fu, V. Robert,V. Tudor, S. Bonnet, and G. F.. Schenider, Adv. Mater. **32**, 1903575 (2020).
[9] M. Gavara-Edo, R. Cordoba, F. J. Valverde-Munoz, J. Herrero-Martin, J. A. Real, and E. Coronado, Adv. Mater. **34**, 2202551 (2022).
[10] M. Gruber and R. Berndt, Magnetochemistry **6**, 35 (2020).
[11] L. Kipgen, M. Bernien, F. Tuczek, and W. Kuch, Adv. Mater. **33**, 2008141 (2021).
[12] T. Jasper-Toennies, M. Gruber, S. Karan, H. Jacob, F. Tuczek, and R. Berndt, J. Phys. Chem. Lett. **8**, 1569 (2017).
[13] C. Fourmental, S. Mondal, R. Banerjee, A. Bellec, Y. Garreau, A. Coati, C. Chacon, Y. Girard, J. Lagoute, S. Rousset, M. L. Boillot, T. Mallah, C. Enachescu, C. Barreteau, Y. J. Dappe, A. Smogunov, S. Narasimhan, and V. Repain, J. Phys. Chem. Lett. **10**, 4103 (2019).
[14] M. Kelai, V. Repain, A. Tauzin, W. B. Li, Y. Girard, J. Lagoute, S. Rousset, E. Otero, P. Sainctavit, M. A. Arrio, M. L. Boillot, T. Mallah, C. Enachescu, and A. Bellec, J. Phys. Chem. Lett. **12**, 6152 (2021).
[15] K. Bairagi, O. Iasco, A. Bellec, A. Kartsev, D. Z. Li, J. Lagoute, C. Chacon, Y. Girard, S. Rousset, F. Miserque, Y. J. Dappe, A. Smogunov, C. Barreteau, M. L. Boillot, T. Mallah, and V. Repain, Nat. Commun. **7**, 12212 (2016).
[16] M. Gruber, V. Davesne, M. Bowen, S. Boukari, E. Beaurepaire, W. Wulfhekel, and T. Miyamachi, Phys. Rev. B **89**, 195415 (2014).
[17] T. Miyamachi, M. Gruber, V. Davesne, M. Bowen, S. Boukari, L. Joly, F. Scheurer, G. Roge, T. K. Yamada, and P. Ohresser, Nat. Commun. **3**, 938 (2012).
[18] T. G. Gopakumar, F. Matino, H. Naggert, A. Bannwarth, F. Tuczek, and R. Berndt, Angew. Chem. Int. Ed. **51**, 6262 (2012).
[19] T. Jasper-Toennies, M. Gruber, S. Karan, H. Jacob, F. Tuczek, and R. Berndt, Nano Lett. **17**, 6613 (2017).
[20] Y. F. Tong, M. Kelai, K. Bairagi, V. Repain, J. Lagoute, Y. Girard, S. Rousset, M. L. Boillot, T. Mallah, C. Enachescu, and A. Bellec, J. Phys. Chem. Lett. **12**, 11029 (2021).
[21] L. Q. Zhang, Y. F. Tong, M. Kelai, A. Bellec, J. M. Lagoute, C. Chacon, Y. Girard, S. Rousset, M. L. Boillot, E. Rivière, T. Mallah, E. Otero, M. A. Arrio, P. Sainctavit, and V. Repain, Angew. Chem. Int. Ed. **59**, 13341 (2020).
[22] K. Affes, A. Slimani, Y. Singh, A. Maalej, and K. Boukheddaden, J. Phys.: Condens. Matter **32**, 255402 (2020).
[23] R. S. de Armas and C. J. Calzado, Inorg. Chem. Front. **9**, 753 (2022).
[24] T. Delgado, C. Enachescu, A. Tissot, L. Guénée, A. Hauser, and C. Besnard, Phys. Chem. Chem. Phys. **20**, 12493 (2018).
[25] C. Enachescu, L. Stoleriu, A. Stancu, and A. Hauser, Phys. Rev. Lett. **102**, 257204 (2009).
[26] C. Enachescu, M. Nishino, S. Miyashita, L. Stoleriu, and A. Stancu, Phys. Rev. B **86**, 054114 (2012).
[27] C. Enachescu and A. Hauser, Phys. Chem. Chem. Phys. **18**, 20591 (2016).
[28] Y. Singh, H. Oubouchou, M. Nishino, S. Miyashita, and K. Boukheddaden, Phys. Rev. B **101**, 054105 (2020).
[29] S. B. Ogou, T. D. Oke, F. Hontinfinde, and K. Boukheddaden, Phys. Rev. B **104**, 024431 (2021).
[30] K. Boukheddaden and A. Bailly-Reyre, Europhys. Lett. **103**, 26005 (2013).
[31] L. Stoleriu, M. Nishino, S. Miyashita, A. Stancu, A. Hauser, and C. Enachescu, Phys. Rev. B **96**, 064115 (2017).
[32] P. Gütlich, A. Hauser, and H. Spiering, Angew. Chem. Int. Ed. Engl. **33**, 2024 (1994).
[33] E. König, in *Complex Chemistry*, Structure and Bonding, Vol. 76 (Springer, Berlin, 1991), p. 51.
[34] C. Enachescu, M. Nishino, S. Miyashita, K. Boukheddaden, F. Varret, and P. A. Rikvold, Phys. Rev. B **91**, 104102 (2015).
[35] A. Tissot, C. Enachescu, and M. L. Boillot, J. Mater. Chem. **22**, 20451 (2012).
[36] C. Enachescu, R. Tanasa, A. Stancu, A. Tissot, J. Laisney, and M. L. Boillot, Appl. Phys. Lett. **109**, 031908 (2016).
[37] S. Fu, J. Yang, and J. F. Lin, Phys. Rev. Lett. **118**, 036402 (2017).
[38] H. Hsu, C. P. Crisostomo, W. Wang, and Z. Wu, Phys. Rev. B **103**, 054401 (2021).
[39] S. Miyashita, P. A. Rikvold, T. Mori, Y. Konishi, M. Nishino, and H. Tokoro, Phys. Rev. B **80**, 064414 (2009).
[40] M. Nishino, C. Enachescu, S. Miyashita, P. A. Rikvold, K. Boukheddaden, and F. Varret, Sci. Rep. **1**, 162 (2011).
[41] C. Enachescu, M. Nishino, S. Miyashita, L. Stoleriu, A. Stancu, and A. Hauser, Europhys. Lett. **91**, 27003 (2010).
[42] A. Slimani, K. Boukheddaden, F. Varret, H. Oubouchou, M. Nishino, and S. Miyashita, Phys. Rev. B **87**, 014111 (2013).
[43] A. Slimani, K. Boukheddaden, F. Varret, M. Nishino, and S. Miyashita, J. Chem. Phys. **139**, 194706 (2013).
[44] F. C. Frank and J. H. van der Merwe, Proc. R. Soc. London A **198**, 205 (1949).
[45] B. Croset and C. de Beauvais, Phys. Rev. B **61**, 3039 (2000).